Geochemical Characterization of Serpentinized Peridotites from the Shergol Ophiolitic Slice along the Indus Suture Zone (ISZ), Ladakh Himalaya, India

Article *in* The Journal of Geology · July 2017

DOI: 10.1086/692653

CITATIONS
16

READS
717

3 authors:

Irfan Maqbool Bhat
University of Kashmir
18 PUBLICATIONS **116** CITATIONS
SEE PROFILE

Talat Ahmad
University of Kashmir
178 PUBLICATIONS **3,705** CITATIONS
SEE PROFILE

D.V. Subba Rao
National Geophysical Research Institute
63 PUBLICATIONS **1,024** CITATIONS
SEE PROFILE

Geochemical Characterization of Serpentinized Peridotites from the Shergol Ophiolitic Slice along the Indus Suture Zone (ISZ), Ladakh Himalaya, India

Irfan Maqbool Bhat,[1,*] *Talat Ahmad,*[2] *and D. V. Subba Rao*[3]

1. Department of Earth Sciences, University of Kashmir, Srinagar 190006, India; 2. Vice Chancellor's Office, Jamia Millia Islamia, New Delhi 110025, India; 3. Geochemistry Division, National Geophysical Research Institute, Hyderabad 500606, India

ABSTRACT

The Shergol ophiolitic slice is a dismembered ophiolite consisting predominantly of serpentinized peridotites along the Indus Suture Zone, Ladakh Himalaya, India. On the basis of modal mineralogy, Shergol serpentinized peridotites can be identified as spinel-bearing harzburgites. The characteristic U-shaped rare earth element (REE) patterns and whole-rock heavy-REE concentrations correspond to those of abyssal mantle rocks from mid-ocean ridges. Evaluation of Cr-spinel mineral chemistry reveals that they represent the residues left after low-to-moderate degrees of partial melting (<15%) in the spinel stability field in a mid-oceanic ridge tectonic environment. The whole-rock geochemistry suggests that the studied rocks represent a mantle residue left after removal of basaltic melts in the context of an ancient Jurassic-Cretaceous Neo-Tethys oceanic mantle section.

Online enhancements: appendix.

Introduction

Ophiolites are the fragments of upper mantle and oceanic crust (i.e., oceanic lithosphere) representing ancient ocean basins (Cann 1970; Dewey and Bird 1971; Coleman 1977; Nicolas 1989) incorporated into continental margins during continent-continent and arc-continent collisions (Dilek and Flower 2003). They are generally found along collisional-type suture zones (e.g., Alpine, Himalayan, Appalachian) and accretionary-type orogenic belts (e.g., North American Cordilleran) that mark major boundaries between amalgamated plates or accreted terranes. The importance of on-land study of ophiolites is immense, as they represent the only suitable source of direct information about the character and composition of the old oceanic lithosphere that will help in understanding the modern oceanic lithosphere.

The ultramafic rocks and other diagnostic lithological types with well-preserved oceanic features that characterize most of the world's known ophiolite sequences occur in the Ladakh Himalaya along the Indus Suture Zone (ISZ; Gansser 1980; Srikantia and Razdan 1980; Sharma 1989; Sinha and Mishra 1992; Mahéo et al. 2004, 2006). This important tectonic setting and its ophiolitic character add to the geological significance of these rocks.

In this article, we present the first whole-rock major- and trace-element compositions, including rare earth element (REE) data, of serpentinized peridotites from the Shergol ophiolitic slice, representing one of the ophiolites of the Ladakh Himalaya along the ISZ. The study also aims at discussing the petrogenesis and tectonic setting of these serpentinized peridotites.

Geological Setting

The Ladakh Himalaya (fig. 1*a*) occupies the central position in the Himalaya; it is separated from the Kohistan area to the west by the Nanga-Parbat massif and is cut off from the Lhasa block to the east by the Karakoram strike-slip fault (Gansser 1980; Srikantia and Razdan 1980; Raz and Honegger 1989).

Manuscript received May 18, 2016; accepted April 6, 2017; electronically published July 14, 2017.

* Author for correspondence; e-mail: imbhat89@gmail.com.

[The Journal of Geology, 2017, volume 125, p. 501–513] 0022-1376/2017/12505-0002$15.00. DOI: 10.1086/692653

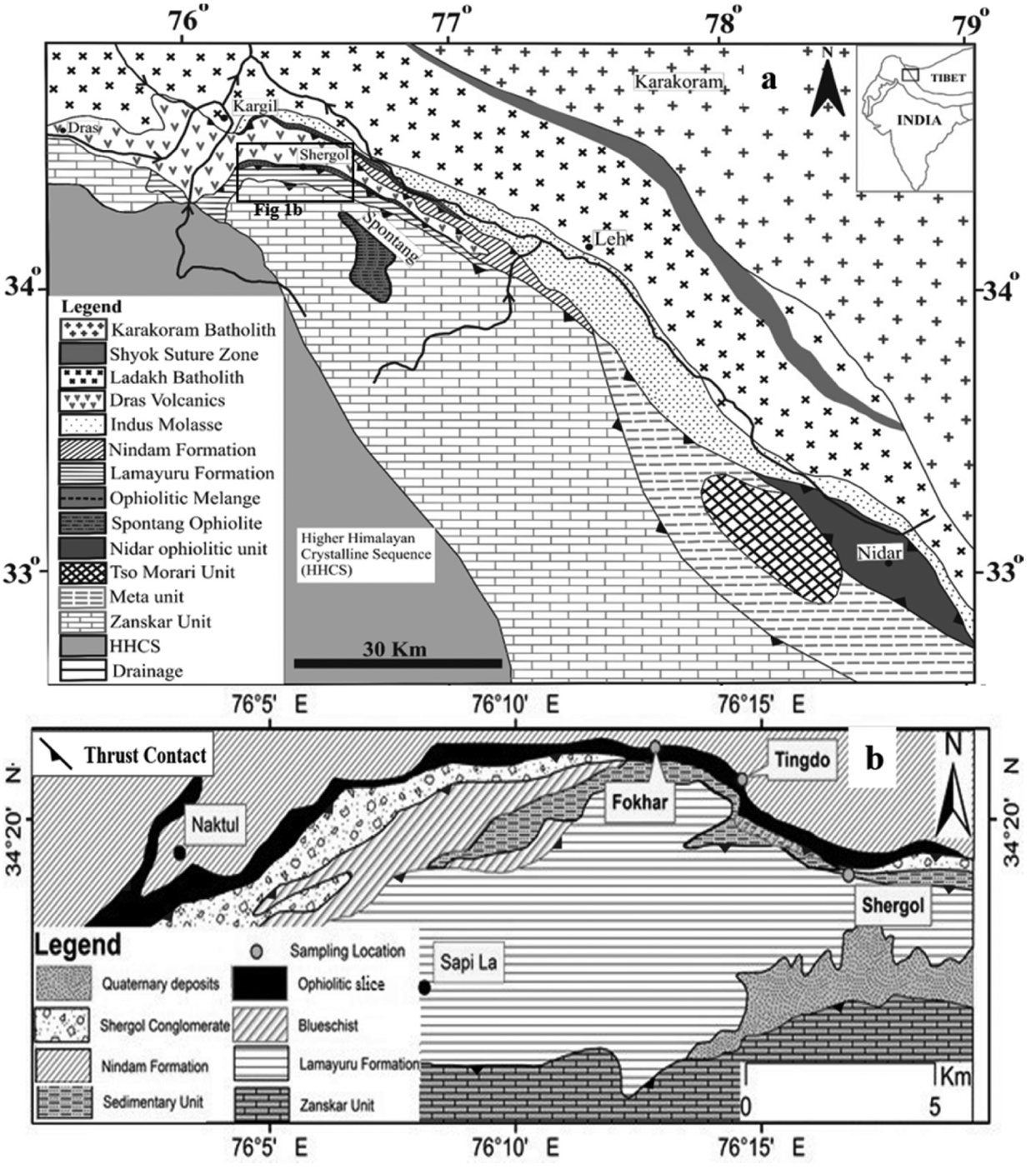

Figure 1. *a*, Geological map of the Ladakh Himalaya (after Mahéo et al. 2004), showing the location of the study area. *b*, Geological map of the Sapi-Shergol ophiolitic slice along the Indus Suture Zone, Ladakh Himalaya, showing sampling locations (modified after Honegger et al. 1989). A color version of this figure is available online.

In the Ladakh Himalaya, the ISZ preserves the vestiges of the Mesozoic Neo-Tethyan Ocean (Gansser 1964, 1980; Petterson and Windley 1985; Sharma 1989; Treloar and Rex 1990; DiPietro and Lawrence 1991; Robertson and Collins 2002; Rolland et al. 2002), which closed via subduction during Early Cretaceous time (Pudsey 1986; Mahéo et al. 2004), followed by obduction of the Neo-Tethyan ophiolites in Kohistan-Ladakh terranes during Late Cretaceous time (Brookfield and Reynolds 1981; Searle et. al. 1999; Corfield

and Searle 2000) and ultimately the collision of two continental plates (Indian and Asian Plates) during Middle Eocene time (Petterson and Windley 1985; Searle et al. 1987; Beck et al. 1996; Rowley 1996). The rocks along the ISZ are mostly deformed as a result of the Tertiary India-Asia collision (Gansser 1964, 1980; Sharma 1989; Treloar and Rex 1990; DiPietro and Lawrence 1991; Robertson and Collins 2002); its associated process of subduction was responsible for the blueschist- and eclogitic-grade metamorphism of rocks (de Sigoyer et al. 1997, 2000; Guillot et al. 2000) constituting the suture-associated mélanges and their emplacement into their present positions (Brookfield and Reynolds 1981; Honegger et al. 1982; Sinha and Mishra 1992; Mahéo et al. 2006). These ophiolitic slices along the ISZ from northwest to southeast are the dismembered ophiolitic slices of Dras and Shergol (Honegger et al. 1982; Radhakrishna et al. 1987; Sinha and Mishra 1994), the Spontang ophiolite complex (Reuber 1986; Corfield et al. 2001), and the Nidar ophiolitic sequence (de Sigoyer et al. 1997; Mahéo et al. 2004; Ahmad et al. 1996, 2008), which are arranged imbricately in an east-west direction and in a tectonic division belonging to the Mesozoic-age Tethyan ophiolitic belt (Moores et al. 2000).

Our geochemical study is on the dismembered Shergol ophiolitic slice, sandwiched between the Nindam Formation, a forearc volcanosedimentary formation of Late Cretaceous to Early Eocene age associated with the Dras arc (Clift et al. 2000), and the Lamayuru Formation, Indian continental slope deposits of Triassic to Cretaceous age (Fuchs 1982; Robertson 2000) on the north and south, respectively, along the south-dipping back thrusts (Frank et al. 1977; Honegger et al. 1989; Sinha and Mishra 1992; Mahéo et al. 2006). This ophiolitic slice is best exposed at Shergol village, 30 km south of the Kargil district, Ladakh Himalaya. The Shergol ophiolitic slice predominantly consists of ultramafic rocks that are mostly serpentinized and occur as long slivers (up to 3 km in length and 200–300 m thick) as well as small blocks (Honegger et al. 1989; Sinha and Mishra 1992, 1994; Robertson 2000). Besides peridotites, the ophiolitic rocks near Shergol village include blueschists, pockets of gabbros, and basalts (Honegger et al. 1982; Sinha and Mishra 1992; Robertson 2000; Mahéo et al. 2006). Despite the presence of all the petrological units of an ophiolite (except for a well-developed sheeted dike complex), these mafic and ultramafic rocks in an accretionary prism at Shergol village are considered to represent a dismembered ophiolite, as regular sequential lithostratigraphy is absent (Shah and Sharma 1977; Srikantia and Razdan 1985; Robertson 2000).

Sampling and Analytical Techniques

For this study, 22 samples of serpentinized peridotite were collected along the trend of the Shergol ophiolitic slice from Shergol village through Tingdo village to Fokhar village (fig. 1*b*). At Shergol village, the ophiolitic slice is confined to an east-west-directed linear belt sandwiched between the Lamayuru Formation on the south and the Nindam Formation on the north, along south-dipping back thrusts (fig. 2*a*). The dominant lithological unit encountered is serpentinized peridotite (harzburgite composition) that mainly occurs as blocks of varying sizes imbricated with a serpentine and turbidite matrix (fig. 2*b*). At Tingdo village (to the west of the Shergol), mafic lenses are intercalated with sheared serpentinized peridotite (fig. 2*c*, 2*d*). These serpentinized peridotites are black to dark green in color, with prominent crystals of shining bronze- or honey-colored platy pseudomorphs of pyroxene (5–8 mm in diameter) known as bastites. After detailed petrographic study, 12 samples were selected for major- and trace-element analyses.

Major-element concentrations were determined with a Philips MagiX PRO (model PW 2440) wavelength-dispersive X-ray fluorescence (XRF) spectrometer coupled with an automatic sample changer (model PW 2540) and provided with suitable software, SUPER Q 3.0 (Philips, Eindhoven, Netherlands). The analytical procedure for major-element determination is essentially the same as that described by Krishna et al. (2007). For all major elements, the precision (relative standard deviation [RSD]) is well below 5% for all samples. Trace elements, including REEs and high-field-strength elements, were determined after digestion of samples with HF-HNO_3 (7:3, acid mixture) in Savillex screw-top vessels. Solutions were analyzed by high-resolution inductively coupled mass spectrometer (ICP-MS; Nu Instruments Attom, Wrexham, United Kingdom) in jump-wiggle mode at a moderate resolution of 300, which permits all the analytes of interest to be measured accurately. The analytical procedure was the same as that followed by Satyanarayanan et al. (2014). The analytical results demonstrate a high degree of machine accuracy and precision better than an RSD of 3% for the majority of trace elements. Major- and trace-element data of Shergol serpentinized peridotites (SSPs) are given in tables A1 and A2, respectively (tables A1–A3 available online).

Electron microprobe analyses of the least-altered peridotite samples were performed at the Banaras Hindu University, Varanasi, India, with a CAMECA SXFive Electron Microprobe. Accelerating voltage and probe current were 15 kV and 20 nA, respec-

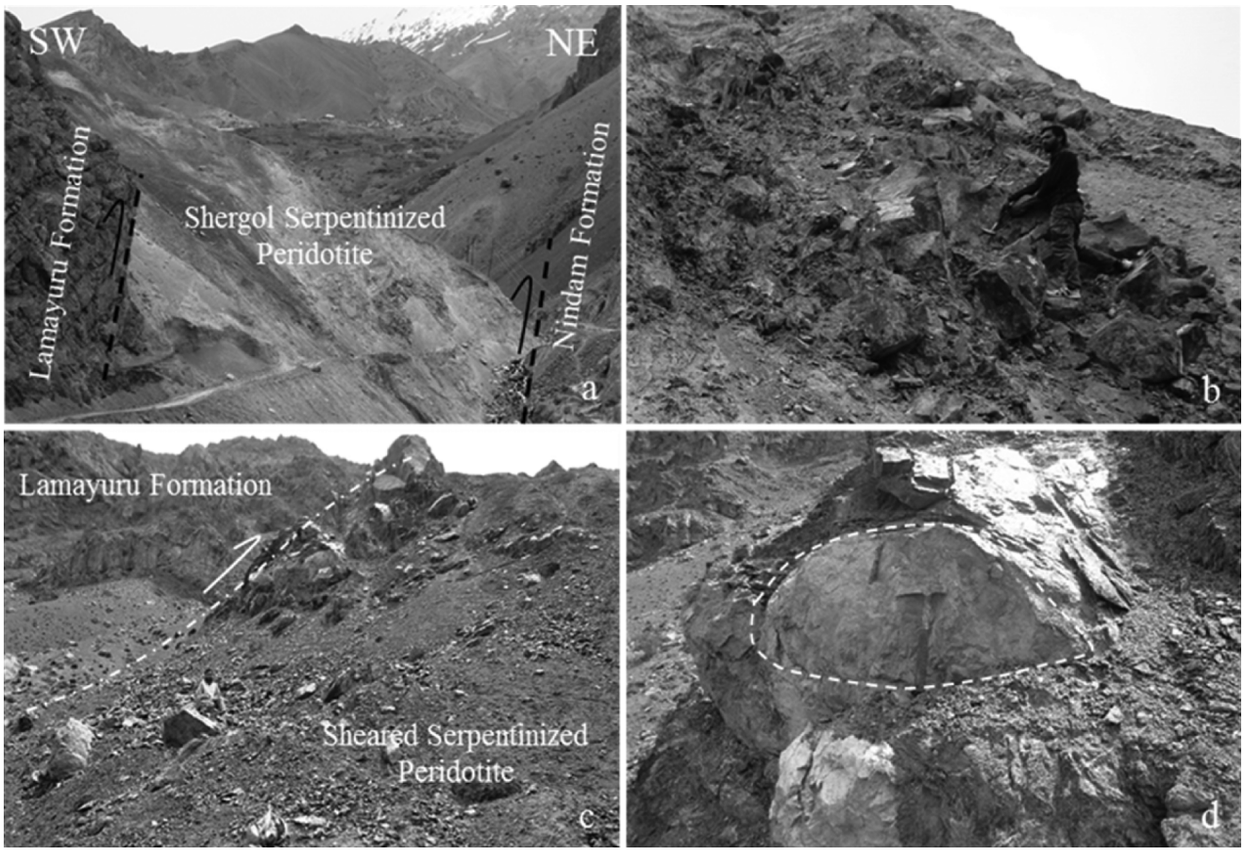

Figure 2. Field photographs of serpentinized peridotites from Shergol ophiolite, Ladakh Himalaya. *a*, Field relation of ophiolitic slice at Shergol village. *b*, Serpentinized peridotite blocks in serpentine matrix. *c*, Outcrop of sheared serpentinized peridotite at Tingdo village. *d*, Mafic lens intercalated with foliated serpentinized peridotite. A color version of this figure is available online.

tively. Well-calibrated natural materials were used as standards, and replicate analyses of individual points show analytical error of <2%. The total Fe was determined as FeO and estimated Fe^{2+} and Fe^{3+} contents, according to the charge-balance equation of Droop (1987). The mineral chemistry of Cr-spinel is presented in table A3.

Results

Petrography. The ultramafic rocks of the Shergol ophiolitic slice at Shergol, Tingdo, and Fokhar villages are invariably serpentinized to varying degrees. Petrographically, these rocks are characterized by pseudomorphic textures, including mesh and hourglass textures after olivine, bastites after orthopyroxene and clinopyroxene, and vein textures of serpentines, besides the presence of accessory amounts of fine-grained magnetite and partly altered characteristic red-brown spinel (fig. 3*a*, 3*b*). Such a mineralogical composition suggests that, before serpentinization, these rocks belonged to a protolith of harzburgite composition. The relict olivine pseudomorphs are anhedral to subhedral grains, measuring from 0.2 to 0.5 mm in diameter, and exhibit hourglass or radial extinction. Orthopyroxene is usually pale brownish and subhedral in shape and commonly occurs as large porphyroclasts of centimeter size. Many orthopyroxene porphyroclasts show undulose extinction, kink banding with minor clinopyroxene exsolution lamellae, chlorite alteration mainly along cleavage planes, and lobate grain boundaries. Spinel grains usually occur as fresh, small, and relatively abundant grains that have characteristic brown to reddish-brown color. These primary spinel grains range from 0.2 to 1 mm in size and are ubiquitously oxidized along grain boundaries, resulting in the development of iron oxide rims, while the red-brown core is preserved (fig. 3*c*, 3*d*).

Whole-Rock Geochemistry. The whole-rock major- and trace-element concentrations of the SSPs are given in tables A1 and A2, respectively. The loss on

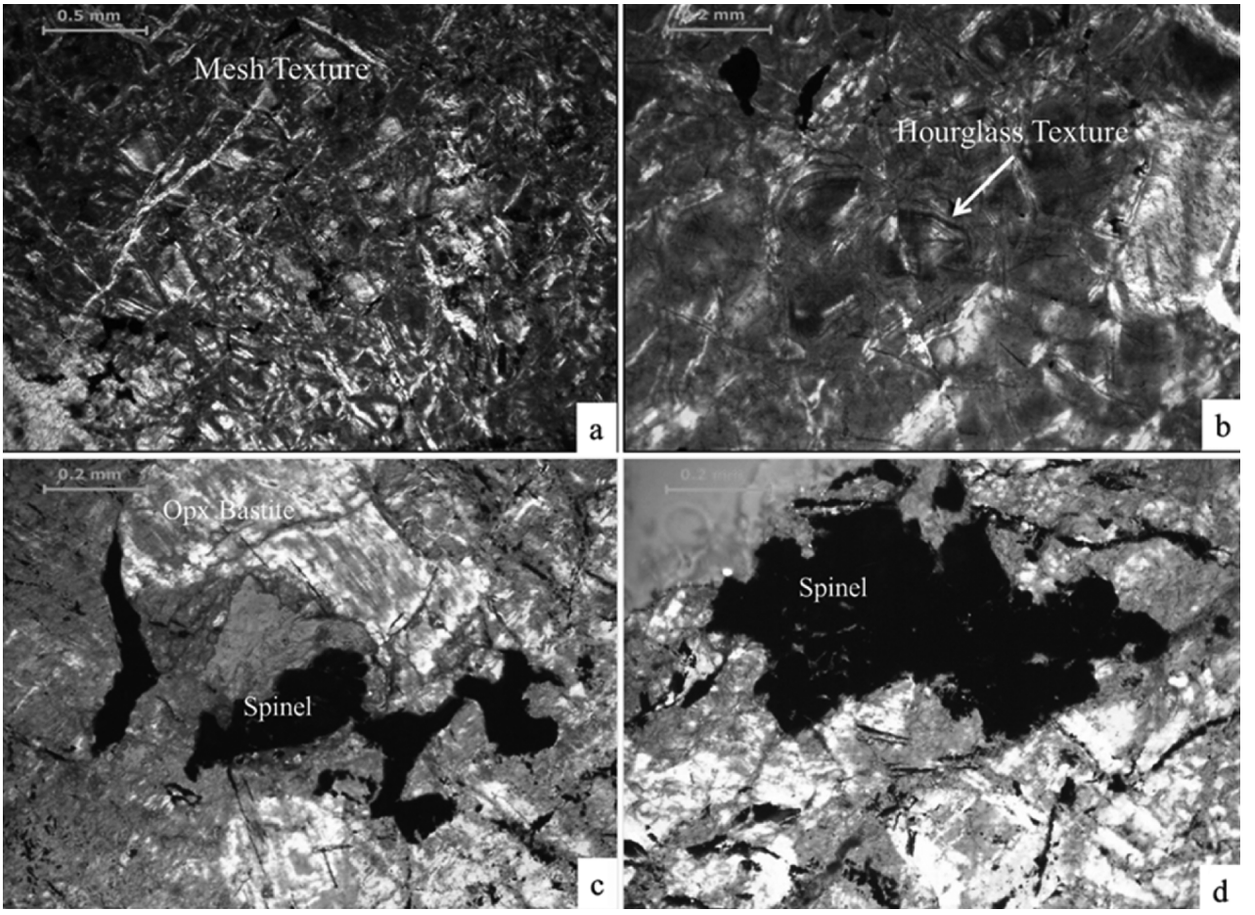

Figure 3. Photomicrographs of the Shergol serpentinized peridotites. *a*, Mesh texture of the peridotite after serpentinization of the ultramafic rock. *b*, Hourglass texture of serpentine pseudomorphs after olivine with characteristic unequal sectors. *c*, Bastite pseudomorphs after orthopyroxene (Opx) and corroded and oxidized spinel grains. *d*, Characteristic oxidized spinel grains with lobate boundary and fine-grained magnetite dust along grain boundaries produced after serpentinization of olivine. A color version of this figure is available online.

ignition (LOI) values range from 6.69 to 14.93 wt%, consistent with the degree of serpentinization (i.e., highly serpentinized samples are characterized by high LOI values, as compared to less serpentinized ones). However, there is not much obvious difference in whole-rock major-element chemistry. The major-element data were recalculated on an anhydrous basis to 100 wt% in order to compensate for variable serpentinization of these peridotites. This normalizing process (recalculating on an anhydrous basis) provides a much better comparison between peridotites having varying amounts of serpentinization (Coleman and Keith 1971; Niu 2004). The degree of serpentinization in peridotites is commonly evaluated by use of LOI values (Deer et al. 1992; Karipi et al. 2006). Generally, highly serpentinized peridotites have high LOI values, as observed in SSPs. The most common major elements susceptible to alteration during serpentinization are Mg, Ca, and Si. The negative correlation of Mg and Si with LOI (fig. 4) and the lack of correlation of Ca, Fe, Ti, and Mn with LOI indicate removal of Mg and Si while the latter elements remain stable in SSPs. The REEs in SSPs show no trend with LOI, indicating that REEs were mostly immobile during alteration.

Among the least mobile elements, Al_2O_3 was used as an index of depletion in order to constrain the behavior of some elements (Snow and Dick 1995). Major elements such as SiO_2, TiO_2, Na_2O, and Fe_2O_3 covary with Al_2O_3, while MgO shows a negative correlation and CaO displays no relation with Al_2O_3 (fig. 5). The more mobile elements, such as large-ion lithophile elements, are unrelated to the depletion index and show similar scatter in SSPs. Thus, the least sensitive or immobile ele-

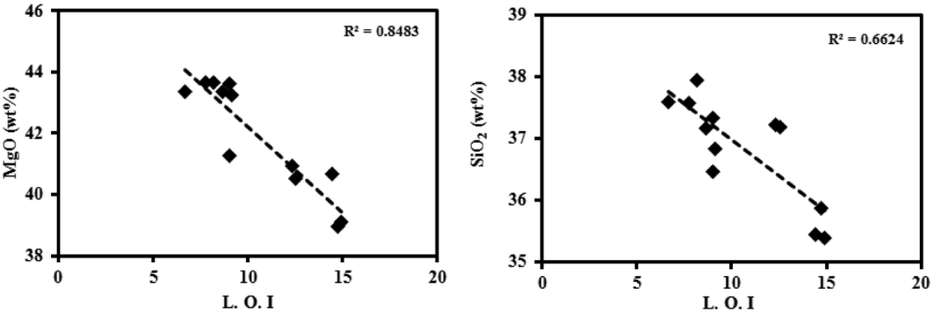

Figure 4. Binary plots of loss on ignition (LOI) versus MgO (*left*) and SiO_2 (*right*), both showing negative correlation with LOI values.

ments were used for geochemical discussion and characterization.

The whole-rock major-element data, when plotted in ACM (Al_2O_3-CaO-MgO) and AFM ((Na_2O + K_2O)-FeO-MgO) ternary diagrams, show that the SSPs correspond to metamorphic peridotites (fig. 6), which, according to Coleman (1977), represent the basal parts of ophiolite sequences, which are depleted or residual mantle rocks. The SSPs are enriched in transition metals such as Ni (1763–2945 ppm), Cr (2997–4727 ppm), Co (94–151 ppm), and Cu (20–91 ppm), reflecting their mantle origin. In a trace-element-versus-Al_2O_3 variation diagram (fig. 7), all the data plot within the field of mantle peridotites (abyssal and ophiolitic) of Bodinier and Godard (2003). Trace elements such as Ni (fig. 7*a*) and Cr (fig. 7*b*) show enrichment with respect to the primitive mantle (PM), as these elements are compatible in mantle minerals (particularly olivine and spinel). Well-defined Zr-versus-Al_2O_3 (fig. 7*c*) and Yb-versus-Al_2O_3 (fig. 7*d*) covariation trends are consistent with tectonically emplaced abyssal peridotites (Bodinier and Godard 2003).

Chondrite-normalized REE patterns of SSPs (fig. 8) are nearly parallel and exhibit convex-downward patterns with a prominent negative Europium anomaly. These rocks are enriched in light REEs relative to middle REEs (MREEs; La_N/Sm_N = 3.11–3.87) and depleted in MREEs relative to heavy REEs (HREEs; Sm_N/Yb_N = 0.21–0.35). This negative Eu anomaly is a result of a primary partitioning event occurring during partial melting, because any impregnation with a hydrothermal fluid would lead to a positive Eu anomaly.

The multielement PM-normalized patterns of SSPs are shown in figure 9. The concentrations of lithophile trace elements in SSPs coincide with those in abyssal peridotites of ocean ridges (Niu 2004), as compared to forearc peridotites (Ishii et al. 1992; Parkinson and Pearce 1998). Cs, Rb, Ba, U, Pb, and Sr display prominent positive spikes, whereas Ta, Zr, Hf, and Eu are depleted relative to Th, as observed in oceanic abyssal peridotites (Niu 2004; Paulick et al. 2006). Also, the depleted REE patterns relative to PM in SSPs are not uncommon and have been observed in orogenic peridotites (Bo-

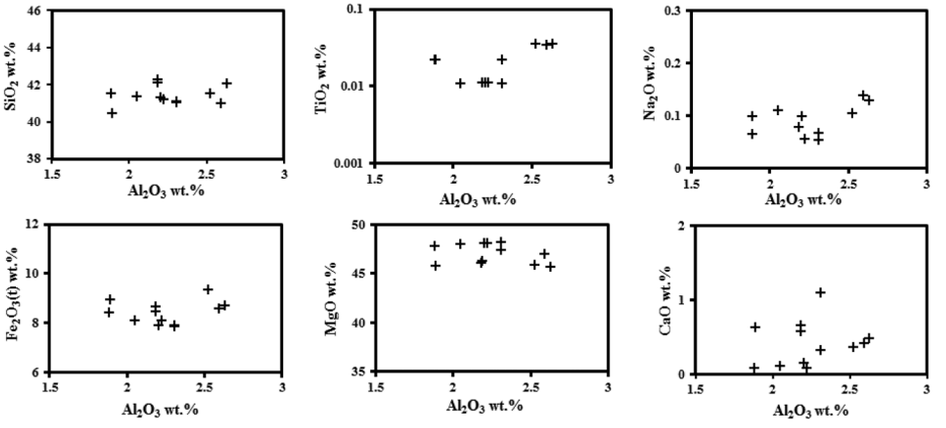

Figure 5. Binary plots of major elements versus Al_2O_3 as depletion index for Shergol serpentinized peridotites.

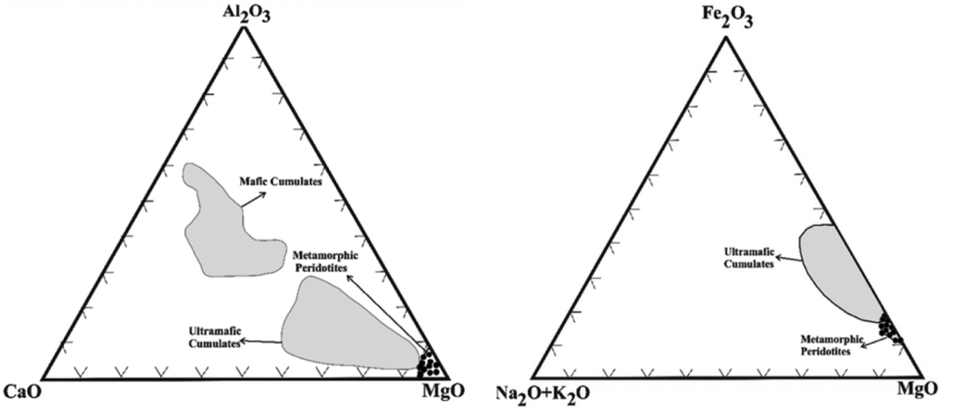

Figure 6. ACM (Al_2O_3-CaO-MgO) and AFM ((Na_2O + K_2O)-FeO-MgO) plots of Shergol serpentinized peridotites. Fields of mafic cumulates, ultramafic cumulates, and metamorphic peridotites are after Coleman (1977). A color version of this figure is available online.

dinier et al. 1990), abyssal peridotites (Niu 2004), and ophiolitic peridotites (Sharma and Wasserburg 1996; Gruau et al. 1998). In ophiolites, the depleted REE patterns are restricted to refractory mantle peridotites (i.e., dunites and harzburgites: Prinzhofer and Allègre 1985; Sharma and Wasserburg 1996) and have been observed in Tethyan ophiolitic peridotites such as those at Othris, Greece (Menzies 1976; Barth et al. 2008); Yarlung Zangbo, Tibet (Dupuis et al. 2005); Trinity, California (Gruau et al. 1998); Samail, Oman (Pallister and Knight 1981; Godard et al. 2000); and Troodos, Cyprus (Kay and Senechal 1976; Taylor and Nesbitt 1988) with their petrogenetic interpretation of being mantle-melting residues.

Mineral Chemistry. The chromian spinel-bearing peridotites from different tectonic environments have distinctive Cr# values, and so can be used to deter-

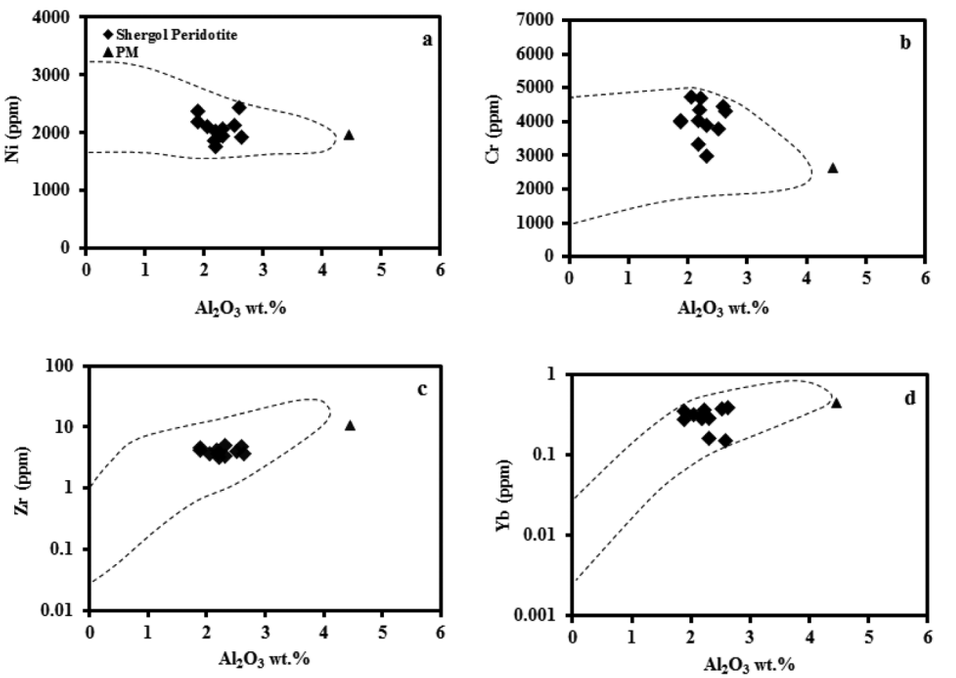

Figure 7. Trace-element oxide covariation with Al_2O_3 (anhydrous wt%) in Shergol serpentinized peridotites. The fields are of orogenic, ophiolitic, and abyssal mantle peridotites (after Bodinier and Godard 2003). Primitive-mantle (PM) values are from McDonough and Sun (1995).

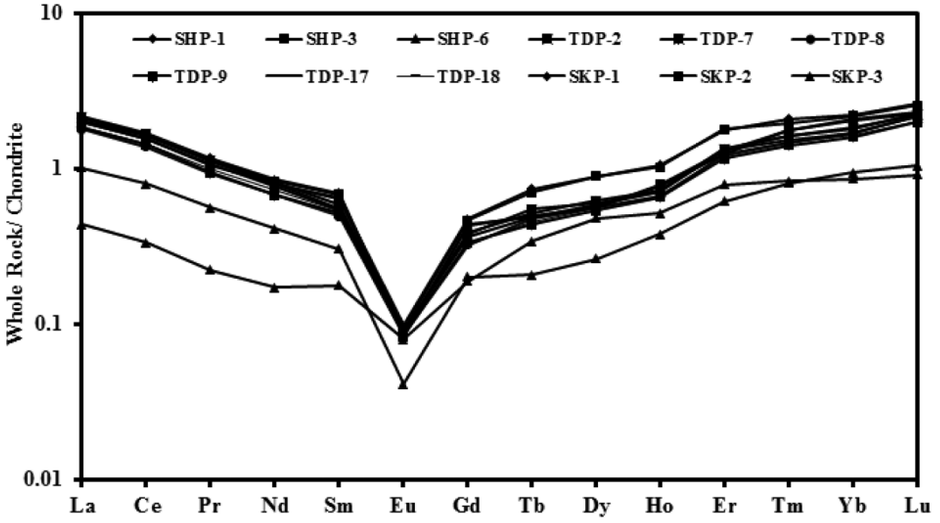

Figure 8. Chondrite-normalized rare earth element patterns of Shergol serpentinized peridotites. Normalizing values are from Sun and McDonough (1989).

mine the degrees of partial melting experienced by the host rock (Dick and Bullen 1984; Arai 1994; Zhou et al. 1996; Hellebrand et al. 2002; Aswad et al. 2011). The Cr-spinels with high Cr# ($Cr^{3+}/(Cr^{3+} + Al^{3+})$ > 0.7) are crystallized from highly magnesian magmas (boninitic type) at the higher partial-melting degrees (>15%) occasionally found in suprasubduction zone environments, whereas lower-Cr# (high-Al) Cr-spinels are precipitated from tholeiitic melts at lower degrees of partial melting (<15%) in mid-ocean ridge environments (Dick and Bullen 1984; Arai 1994; Zhou et al. 1996).

The chemistry of Cr-spinel in SSPs is characterized by low Cr_2O_3 (28.86–32.59 wt%) and high Al_2O_3 (33.76–37.71 wt%). These Cr-spinels have narrow ranges of FeO (from 11.93 to 14.54 wt%) and MgO (from 13.78 to 15.85 wt%; table A3). In these peridotites, the Cr# and Al# ($Al^{3+}/(Cr^{3+} + Al^{3+} + Fe^{3+})$) range from 0.34 to 0.39 and from 0.58 to 0.64, respectively, and are comparable to those observed in Cr-spinel of abyssal peridotites (Dick and Bullen 1984; Arai 1992). The TiO_2 contents (0.02–0.28) of Cr-spinel are also comparable to those of the mid-oceanic ridge tholeiites. The lower Fe# ($Fe^{3+}/(Cr^{3+} + Al^{3+} + Fe^{3+})$),

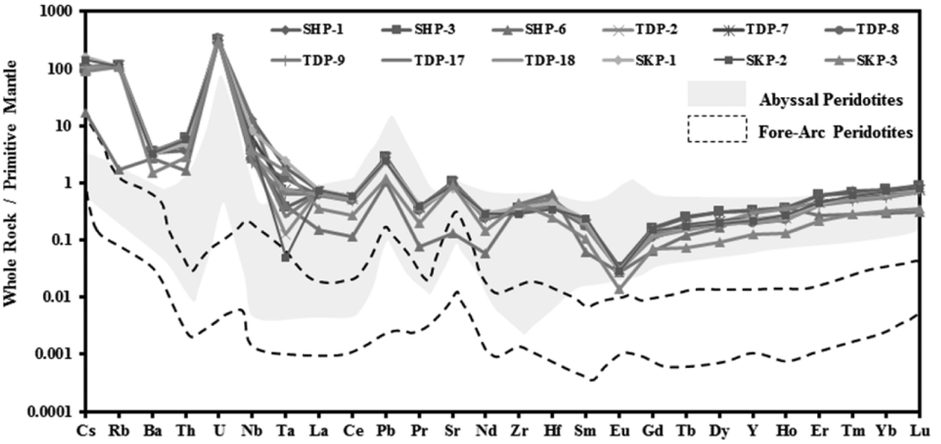

Figure 9. Primitive mantle (PM)–normalized multielement patterns in Shergol serpentinized peridotites (whole-rock analyses). Fields of abyssal peridotites (gray) and forearc peridotites (dashed line area) are from Niu (2004) and Parkinson et al. (1992), respectively. The PM-normalizing values are from Sun and McDonough (1989). A color version of this figure is available online.

ranging from 0.37 to 0.69, and the lower ratio of Fe^{2+}/Fe^{3+}, ranging from 2.13 to 4.53 in the Cr-spinel, suggest that they formed at lower fO_2.

Discussion

Origin of the SSPs. The depletion of bulk-rock major and trace elements, relative to PM values, and the convex-downward chondrite-normalized REE patterns of SSPs indicate that their melting-residual nature resulted from extraction of basaltic melts. The higher average value of Al_2O_3 (2.26 anhydrous wt%) in the studied samples, relative to that of normal ophiolitic harzburgites and dunites, reflects the moderately refractory nature, similar to abyssal peridotites of mid-ocean ridge setting (Coleman 1971; Niu 1997, 2004; Niu and Hékinian 1997; Niu et al. 1997). In order to constrain the nature of the protolith for SSPs, we focused on the HREEs, which are insensitive to or little disturbed by postmelting processes (Kogiso et al. 1997; Canil 2004; Niu 2004; Iyer et al. 2008; Deschamps et al. 2010). Our results suggest that SSPs have REE contents (particularly highly immobile HREE contents) that are similar to those of serpentinized peridotites from mid-ocean ridges (abyssal peridotites) and at least one order of magnitude higher than those found in forearc-depleted peridotites from subduction zones (fig. 9). This protolith signature of the studied rocks is also evident from the Al_2O_3-versus-Yb variation diagram (fig. 7*d*), which reflects that the original geodynamic setting of the SSPs is similar to that of mid-ocean ridge abyssal peridotites.

Parental Melt Generation. In order to understand the primary mantle melting processes in SSPs, we focused on the elements least remobilized by fluids. The HREEs (particularly Yb) are mildly incompatible in mantle mineralogy and are insensitive to postmelting processes and hydrothermal alterations (Bodinier et al. 1990; You et al. 1996; Bedini and Bodinier 1999; Canil 2004; Deschamps et al. 2010). The SSPs exhibit a mildly fertile mantle signature, which is evident from their high whole-rock Al_2O_3 ($1.88 < Al_2O_3$ anhydrous wt% < 2.63) and HREE ($0.9 < Yb_N < 2.2$) concentrations. As observed from petrographic study, there is no primary and/or metamorphic plagioclase or garnet present in the SSPs. However, spinel is present as an aluminous phase, which indicates the equilibrium of SSPs in the spinel stability field. The degrees of partial melting of mantle peridotites can be evaluated by using the melting-model equation $F = 10 \times \ln(\mathrm{Cr}) + 24$ proposed by Hellebrand et al. (2001), where F is melting degrees (in percent). The calculated melting-degree values of SSPs range from 13% to 14% (table A3), indicating that the SSPs experienced <15% partial melting in the spinel stability field.

Tectonic Setting of the SSPs. The primary core compositions of Cr-spinels of SSPs are plotted in various discrimination diagrams (fig. 10) in order to examine their primary igneous characteristics and to determine their tectonic setting. In the Al_2O_3-versus-TiO_2 plot (fig. 10*a*) and the Al_2O_3-versus-Fe^{2+}/Fe^{3+} plot (fig. 10*b*), the SSPs, in comparison to modern-day tectonic settings, are clustered in the mid-ocean ridge peridotite field. In the Mg#-versus-Cr# diagram (fig. 10*c*), the SSPs plot in the lower end of abyssal peridotite field, indicative of their depleted nature (Arai 1994), and reflect <15% partial melting based on the formulation of Hirose and Kawamoto (1995). The SSP spinel compositions are consistent with worldwide abyssal peridotite spinels and suggest that their parent peridotites underwent relatively low fractions of melt extraction (<15% melting), based on the correlation between Cr# and the degree of melting from the modeled equation of Hellebrand et al. (2001; table A3). The enrichment of large-ion lithophile elements (Rb, Ba, Cs, Th, U, and Pb) in SSPs can be attributed to continental sources, while they were incorporated into crustal regions during emplacement along the ISZ as a result of the Cenozoic collision of the Indian and Asian continental margins. Similar enrichments were observed in the Nehbandan ophiolitic peridotites of eastern Iran (Delavari et al. 2009), abyssal peridotites of the Manipur Ophiolite Complex (Ningthoujam et al. 2012; Singh 2013), the Massif du Sud ophiolite in New Caledonia (Marchesi et al. 2009), and the Cerro del Almirez ultramafic massif of southern Spain (Marchesi et al. 2013). Together, these data indicate that the SSPs were formed in a mid-oceanic ridge tectonic setting, instead of a suprasubduction zone setting (Kamenetsky et al. 2001).

Conclusion

Shergol serpentinized peridotites can be grouped as accretionary-type ophiolites, since they occur in a subduction-accretionary complex along the ISZ in the northwestern Himalaya. Results suggest that these rocks originated as melting residues remaining after low-to-moderate degrees of partial melting (<15%) of moderately fertile lherzolite in the spinel stability field in a mid-oceanic ridge tectonic setting. The presence of solid-state deformation textures, refractory chemistry, and whole-rock depleted REE abundances with characteristic convex-downward normalized REE patterns gives credence to this conclusion. It is thus proposed that the SSPs

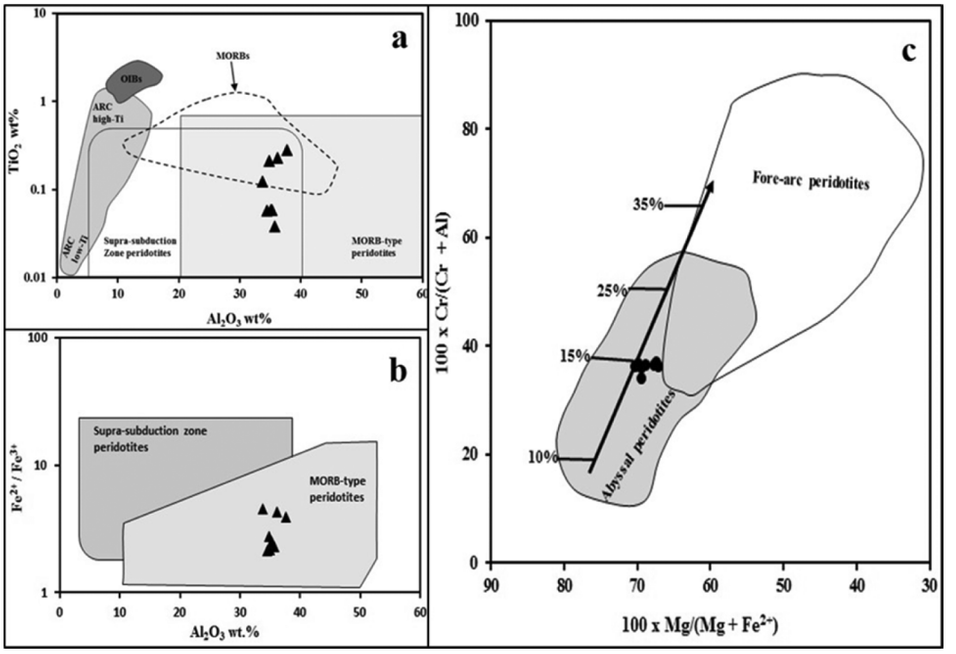

Figure 10. Plots of Cr-spinel compositions. *a*, *b*, Al_2O_3-versus-TiO_2 (*a*) and Al_2O_3-versus-Fe^{2+}/Fe^{3+} (*b*) plots (after Kamenetsky et al. 2001) of Cr-spinels from Shergol peridotites in comparison to modern-day tectonic settings. *c*, Mg# versus Cr#; abyssal and forearc peridotite fields are from Dick and Bullen (1984) and Ishii et al. (1992), respectively. The arrow reflecting the percentage of partial melting is from Hirose and Kawamoto (1995). ARC = island-arc basalt; MORB = mid-ocean ridge basalt; OIB = oceanic island basalt.

represent a portion of ancient Neo-Tethyan oceanic lithospheric mantle that originally developed in a mid-ocean ridge tectonic setting and was subsequently trapped in the accretionary complex of the Ladakh magmatic arc but was not significantly modified by subduction processes before emplacement at its present position.

ACKNOWLEDGMENTS

This work was supported by the Council of Scientific and Industrial Research (CSIR, New Delhi) under a junior research fellowship (JRF) grant to I. M. Bhat. We are thankful to the head of the Department of Earth Sciences, University of Kashmir, for providing facilities to carry out this work. The help extended by M. Satyanarayanan, K. Subramanyam, and A. K. Krishna during ICP-MS and XRF analysis at the National Geophysical Research Institute, Hyderabad, India, is thankfully acknowledged. N. V. Chalapathi Rao, of Banaras Hindu University, Varanasi, India, is kindly thanked for mineral chemistry analysis. Constructive comments and valuable suggestions from reviewers S. Guillot and G. Mahéo are highly acknowledged.

REFERENCES CITED

Ahmad, T.; Islam, R.; Khanna, P. P.; and Thakur, V. C. 1996. Geochemistry, petrogenesis and tectonic significance of the basic volcanic units of the Zildat ophiolitic mélange, Indus suture zone, eastern Ladakh (India). Geodin. Acta 9:222–233.

Ahmad, T.; Tanaka, T.; Sachan, H. K.; Asahara, Y.; Islam, R.; and Khanna, P. P. 2008. Geochemical and isotopic constraints on the age and origin of the Nidar Ophiolitic Complex, Ladakh, India: implications for the Neo-Tethyan subduction along the Indus suture zone. Tectonophysics 451:206–224.

Arai, S. 1992. Chemistry of chromian spinel in volcanic rocks as a potential guide to magma chemistry. Mineral. Mag. 56:173–184.

———. 1994. Characterization of spinel peridotites by olivine-spinel compositional relationships: review and interpretation. Chem. Geol. 113:191–204.

Aswad, K. J.; Aziz, N. R.; and Koyi, H. A. 2011. Cr-spinel compositions in serpentinites and their implications for the petrotectonic history of the Zagros Suture Zone, Kurdistan Region, Iraq. Geol. Mag. 148:802–818.

Barth, M. G.; Mason, P. R. D.; Davies, G. R.; and Drury, M. R. 2008. The Othris Ophiolite, Greece: a snapshot of subduction initiation at a mid-ocean ridge. Lithos 100:234–254.

Beck, R. A.; Burbank, W.; Sercombe, W. J.; Khan, A. M.; and Lawrence, R. D. 1996. Late Cretaceous ophiolite obduction and Paleocene India-Asia collision in the westernmost Himalaya. Geodin. Acta 9:114–144.

Bedini, R. M., and Bodinier, J.-L. 1999. Distribution of incompatible trace elements between the constituents of spinel peridotite xenoliths: ICP-MS data from the East African Rift. Geochim. Cosmochim. Acta 63:3883–3900.

Bodinier, J.-L., and Godard, M. 2003. Orogenic, ophiolitic, and abyssal peridotites. *In* Carlson, R. W., ed. Treatise on geochemistry. Vol. 2. The mantle and core. Amsterdam, Elsevier, p. 103–170.

Bodinier, J. L.; Vasseur, G.; Vernières, J.; Dupuy, C.; and Fabriès, J. 1990. Mechanism of mantle metasomatism: geochemical evidence from the Lherz orogenic peridotite. J. Petrol. 31:597–628.

Brookfield, M. E., and Reynolds, P. H. 1981. Late Cretaceous emplacement of the Indus suture zone ophiolitic mélanges and an Eocene-Oligocene magmatic arc on the northern edge of the Indian plate. Earth Planet. Sci. Lett. 55:157–162.

Canil, D. 2004. Mildly incompatible elements in peridotites and the origins of mantle lithosphere. Lithos 77:375–393.

Cann, J. R. 1970. New model for the structure of the ocean crust. Nature 226:928–930.

Clift, P. D.; Degnan, P. J.; Hannigan, R.; and Blusztajn, J. 2000. Sedimentary and geochemical evolution of the Dras forearc basin, Indus suture, Ladakh Himalaya, India. Geol. Soc. Am. Bull. 112:450–466.

Coleman, R. G. 1971. Plate tectonic emplacement of upper mantle peridotites along continental edges. J. Geophys. Res. 76:1212–1222.

———. 1977. Ophiolites: ancient continental lithosphere? New York, Springer, 220 p.

Coleman, R. G., and Keith, T. E. 1971. A chemical study of serpentinization—Burro Mountain, California. J. Petrol. 12:311–328.

Corfield, R. I., and Searle, M. P. 2000. Crustal shortening estimates across the north Indian continental margin, Ladakh, NW India. *In* Khan, M. A.; Treloar, P. J.; Searle, M. P.; and Khan, M. Q., eds. Tectonics of the Nanga Parbat syntaxis and the western Himalaya. Geol. Soc. Lond. Spec. Publ. 170:395–410.

Corfield, R. I.; Searle, M. P.; and Pedersen, R. B. 2001. Tectonic setting, origin, and obduction history of the Spontang ophiolite, Ladakh Himalaya, NW India. J. Geol. 109:715–736.

Deer, W. R.; Howie, R. A.; and Zussman, J. 1992. An introduction to the rock-forming minerals (2nd ed.). Harlow, UK, Longman.

Delavari, M.; Amini, S.; Saccani, E.; and Beccaluva, L. 2009. Geochemistry and petrogenesis of mantle peridotites from the Nehbandan Ophiolitic Complex, eastern Iran. J. Appl. Sci. 9:2671–2687.

Deschamps, F.; Guillot, S.; Godard, M.; Chauvel, C.; Andreani, M.; and Hattori, K. 2010. In situ characterization of serpentinites from forearc mantle wedges: timing of serpentinization and behavior of fluid-mobile elements in subduction zones. Chem. Geol. 269:262–277.

de Sigoyer, J.; Chavagnac, V.; Blichert-Toft, J.; Villa, I. M.; Luais, B.; Guillot, S.; Cosca, M.; and Mascle, G. 2000. Dating the Indian continental subduction and collisional thickening in the northwest Himalaya: multichronology of the Tso Morari eclogites. Geology 28: 487–490.

de Sigoyer, J.; Guillot, S.; Lardeaux, J. M.; and Mascle, G. 1997. Glaucophane bearing eclogites in the Tso Morari dome (eastern Ladakh, NW Himalaya). Eur. J. Mineral. 9:1073–1083.

Dewey, J. F., and Bird, J. M. 1971. Origin and emplacement of the ophiolite suite: Appalachian ophiolites in Newfoundland. J. Geophys. Res. 76:3179–3206.

Dick, H. J. B., and Bullen, T. 1984. Cr-spinel as a petrogenetic indicator in abyssal and alpine-type peridotites and spatially associated lavas. Contrib. Mineral. Petrol. 86:54–76.

Dilek, Y., and Flower, M. F. J. 2003. Arc-trench roll back and forearc accretion: 2. A model template for ophiolites in Albania, Cyprus, and Oman. *In* Dilek, Y., and Robinson, P. T., eds. Ophiolites in earth history. Geol. Soc. Lond. Spec. Publ. 218:43–68.

DiPietro, J. A., and Lawrence, R. D. 1991. Himalayan structure and metamorphism south of the Main Mantle Thrust, Lower Swat, Pakistan. J. Metamorph. Geol. 9:481–495.

Droop, G. T. R. 1987. A general equation for estimating Fe^{3+} concentrations in ferromagnesian silicates and oxides from microprobe analyses, using stoichiometric criteria. Mineral. Mag. 51:431–435.

Dupuis, C.; Hébert, R.; Dubois-Côté, V.; Guilmette, C.; Wang, C. S.; Li, Y. L.; and Li, Z. J. 2005. The Yarlung Zangbo Suture Zone ophiolitic mélange (southern Tibet): new insights from geochemistry of ultramafic rocks. J. Asian Earth Sci. 25:937–960.

Frank, W.; Gansser, A.; and Trommsdorff, V. 1977. Geological observations in the Ladakh area (Himalayas)—a preliminary report. Schweiz. Mineral. Petrograph. Mitt. 57:89–113.

Fuchs, G. 1982. The geology of the Pin valley in Spiti, H. P., India. Jahrb. Geol. Bundesanst. 124:325–359.

Gansser, A. 1964. The geology of the Himalayas. New York, Wiley-Interscience, 289 p.

———. 1980. The significance of the Himalaya suture zone. Tectonophysics 62:37–40.

Godard, M.; Jousselin, D.; and Bodinier, J.-L. 2000. Relationships between geochemistry and structure beneath a palaeo-spreading centre: a study of the mantle section in the Oman ophiolite. Earth Planet. Sci. Lett. 180:133–148.

Gruau, G.; Bernard-Griffiths, J.; and Lecuyer, C. 1998. The origin of U-shaped rare earth patterns in ophiolite peridotites: assessing the role of secondary alteration and melt/rock reaction. Geochim. Cosmochim. Acta 62:3545–3560.

Guillot, S.; Hattori, K. H.; and de Sigoyer, J. 2000. Mantle wedge serpentinization and exhumation of eclogites: insights from eastern Ladakh, NW Himalaya. Geology 28:199–202.

Hellebrand, E.; Snow, J. E.; Dick, H. J. B.; and Hofmann, A. W. 2001. Coupled major and trace elements as indicators of the extent of melting in the mid-ocean-ridge peridotites. Nature 410:677–681.

Hellebrand, E.; Snow, J. E.; Hoppe, P.; and Hofmann, A. 2002. Garnet-field melting and late-stage refertilization in 'residual' abyssal peridotites from the Central Indian Ridge. J. Petrol. 43:2305–2338.

Hirose, K., and Kawamoto, T. 1995. Hydrous partial melting of lherzolite at 1 Gpa: the effect of H_2O on the genesis of basaltic magmas. Earth Planet. Sci. Lett. 133: 463–473.

Honegger, K.; Dietrich, V.; Frank, W.; Gansser, A.; Thöni, M.; and Trommsdorf, V. 1982. Magmatic and metamorphism in the Ladakh Himalayas (the Indus-Tsangpo suture zone). Earth Planet. Sci. Lett. 60:253–292.

Honegger, K.; Le Fort, P.; Mascle, G.; and Zimmermann, J. L. 1989. The blueschists along the Indus Suture Zone in Ladakh, NW Himalaya. J. Metamorph. Geol. 7:57–72.

Ishii, T.; Robinson, P. T.; Mackawa, H.; and Fiske, R. 1992. Petrological studies of peridotites from diapiric serpentinite seamounts in the Izu-Ogazawara-Mariana forearc, Leg 125. *In* Proc. ODP, Sci. Results 125. College Station, TX, Ocean Drilling Program, p. 445–485.

Iyer, K.; Austrheim, H.; John, T.; and Jamtveit, B. 2008. Serpentinization of the oceanic lithosphere and some geochemical consequences: constraints from the Leka Ophiolite Complex, Norway. Chem. Geol. 249:66–90.

Kamenetsky, V. S.; Crawford, A. J.; and Meffre, S. 2001. Factors controlling chemistry of magmatic spinel: an empirical study of associated olivine, Cr-spinel and melt inclusions from primitive rocks. J. Petrol. 42:655–671.

Karipi, S.; Tsikouras, B.; and Hatzipanagiotou, K. 2006. The petrogenesis and tectonic setting of ultramafic rocks from Iti and Kallidromon Mountains, continental central Greece: vestiges of the Pindos Ocean. Can. Mineral. 44:267–287.

Kay, R. W., and Senechal, R. G. 1976. The rare earth chemistry of the Troodos Ophiolite Complex. J. Geophys. Res. 81:964–970.

Kogiso, T.; Tatsumi, Y.; and Nakano, S. 1997. Trace element transport during dehydration processes in the subducted oceanic crust: 1. Experiments and implications for the origin of ocean island basalts. Earth Planet. Sci. Lett. 148:193–205.

Krishna, A. K.; Murthy, N. N.; and Govil, P. K. 2007. Multi-element analysis of soils by wavelength-dispersive X-ray fluorescence spectrometry. At. Spectrosc. 28(6): 202–214.

Mahéo, G.; Bertrand, H.; Guillot, S.; Villa, I. M.; Keller, F.; and Capiez, P. 2004. The south Ladakh ophiolites (NW Himalaya, India): an intra-oceanic tholeiitic origin with implication for the closure of the Neo-Tethys. Chem. Geol. 203:273–303.

Mahéo, G.; Fayoux, X.; Guillot, S.; Garzanti, E.; Capiez, P.; and Mascle, G. 2006. Relicts of an intra-oceanic arc in the Sapi-Shergol mélange zone (Ladakh, NW Himalaya, India): implications for the closure of the Neo-Tethys Ocean. J. Asian Earth Sci. 26:695–707.

Marchesi, C.; Garrido, C.; Godard, M.; Belley, F.; and Ferré, E. 2009. Migration and accumulation of ultra-depleted subduction-related melts in the Massif du Sud ophiolite (New Caledonia). Chem. Geol. 266:171–186.

Marchesi, C.; Garrido, C. J.; Padrón-Navarta, J. A.; López Sánchez-Vizcaíno, V.; and Gómez-Pugnaire, M. T. 2013. Element mobility from seafloor serpentinization to high-pressure dehydration of antigorite in subduction serpentinite: insights from the Cerro del Almirez ultramafic massif (southern Spain). Lithos 178:128–142.

McDonough, W. F., and Sun, S. S. 1995. The composition of the Earth. Chem. Geol. 120:223–253.

Menzies, M. 1976. Rare earth geochemistry of fused ophiolitic and alpine lherzolites—I. Othris, Lanzo and Troodos. Geochim. Cosmochim. Acta 40:645–656.

Moores, E. M.; Kellogg, L. H.; and Dilek, Y. 2000. Tethyan ophiolites, mantle convection, and tectonic "historical contingency": a resolution of the "ophiolite conundrum." *In* Dilek, Y.; Moores, E. M.; Elthon, D.; and Nicolas, A., eds. Ophiolites and oceanic crust: new insights from field studies and the Ocean Drilling Program. Geol. Soc. Am. Spec. Pap. 349:3–12.

Nicolas, A. 1989. Structure of ophiolites and dynamics of oceanic lithosphere. Dordrecht, Kluwer Academic, 368 p.

Ningthoujam, P. S.; Dubey, C. S.; Guillot, S.; Fagio, A. S.; and Shukla, D. P. 2012. Origin and serpentinization of ultramafic rocks of Manipur Ophiolite Complex in the Indo-Myanmar subduction zone, northeast India. J. Asian Earth Sci. 50:128–140.

Niu, Y. 1997. Mantle melting and melt extraction processes beneath ocean ridges: evidence from abyssal peridotites. J. Petrol. 38:1047–1074.

———. 2004. Bulk-rock major and trace element compositions of abyssal peridotites: implications for mantle melting, melt extraction and post-melting processes beneath mid-ocean ridges. J. Petrol. 45:2423–2458.

Niu, Y., and Hékinian, R. 1997. Basaltic liquids and harzburgitic residues in the Garrett Transform: a case study at fast-spreading ridges. Earth Planet. Sci. Lett. 146:243–258.

Niu, Y.; Langmuir, C. H.; and Kinzler, R. J. 1997. The origin of abyssal peridotites: a new perspective. Earth Planet. Sci. Lett. 152:251–265.

Pallister, J. S., and Knight, R. J. 1981. Rare-earth element geochemistry of the Samail ophiolite near Ibra, Oman. J. Geophys. Res. 86(B4):2673–2697.

Parkinson, I. J., and Pearce, J. A. 1998. Peridotites from the Izu-Bonin-Mariana forearc (ODP Leg 125): evidence for mantle melting and mantle-melt interaction in a supra-subduction zone setting. J. Petrol. 39:1577–1618.

Parkinson, I. J.; Pearce, J. A.; Thirlwall, M. F.; Johnson, K. T. M.; and Ingram, G. 1992. Trace element geochemistry of peridotites from the Izu-Bonin-Mariana forearc, Leg 125. *In* Proc. ODP, Sci. Results 125. College Station, TX, Ocean Drilling Program, p. 487–506.

Paulick, H.; Bach, W.; Godard, M.; De Hoog, J. C. M.; Suhr, G.; and Harvey, J. 2006. Geochemistry of abyssal peridotites (Mid-Atlantic Ridge, 15°20′N, ODP Leg 209): implications for fluid/rock interaction in slow spreading environments. Chem. Geol. 234:179–210.

Petterson, M. G., and Windley, B. F. 1985. Rb-Sr dating of the Kohistan arc-batholith in the Trans-Himalaya of north Pakistan and tectonic implications. Earth Planet. Sci. Lett. 74:45–75.

Prinzhofer, A., and Allègre, C. J. 1985. Residual peridotites and the mechanisms of partial melting. Earth Planet. Sci. Lett. 74:251–265.

Pudsey, C. J. 1986. The Northern Suture, Pakistan: margin of a Cretaceous island arc. Geol. Mag. 123:405–423.

Radhakrishna, T.; Divakara Rao, V.; and Murali, A. V. 1987. Geochemistry and petrogenesis of ultramafic and mafic plutonic rocks of the Dras ophiolitic melange, Indus suture (northwest Himalaya). Earth Planet. Sci. Lett. 82:136–144.

Raz, U., and Honegger, K. 1989. Magmatic and tectonic evolution of the Ladakh Block from field studies. Tectonophysics 161:107–118.

Reuber, I. 1986. Geometry of accretion and oceanic thrusting of Spontang ophiolite, Ladakh-Himalaya. Nature 321:592–596.

Robertson, A. H. F. 2000. Formation of mélanges in the Indus Suture Zone, Ladakh Himalaya by successive subduction-related, collisional and post-collisional processes during Late Mesozoic–Late Tertiary time. *In* Khan, M. A.; Treloar, P. J.; Searle, M. P.; and Khan, M. Q., eds. Tectonics of the Nanga Parbat syntaxis and the western Himalaya. Geol. Soc. Lond. Spec. Publ. 170:333–374.

Robertson, A. H. F., and Collins, A. S. 2002. Shyok Suture Zone, N Pakistan: late Mesozoic-Tertiary evolution of a critical suture separating the oceanic Ladakh Arc from the Asian continental margin. J. Asian Earth Sci. 20:309–351.

Rolland, Y.; Picard, C.; Pecher, A.; Lapierre, H.; Bosch, D.; and Keller, F. 2002. The Cretaceous Ladakh arc of NW Himalaya—slab melting and melt-mantle interaction during fast northward drift of Indian Plate. Chem. Geol. 182:139–178.

Rowley, D. B. 1996. Age of initiation of collision between India and Asia: a review of stratigraphic data. Earth Planet. Sci. Lett. 145:1–13.

Satyanarayanan, M.; Balaram, V.; Sawant, S. S.; Subramanyam, K. S. V.; and Krishna, G. V. 2014. High precision multielement analysis on geological samples by HR-ICP-MS. *In* ISMAS-WS (Indian Society for Mass Spectrometry Symposium cum workshop on Mass Spectrometry), 28th. Proc. Parwanoo, ISMAS, p. 181–184.

Searle, M. P.; Khan, M. A.; Fraser, J. E.; and Gough, S. J. 1999. The tectonic evolution of the Kohistan-Karakoram collision belt along the Karakoram Highway transect, north Pakistan. Tectonics 18:929–949.

Searle, M. P.; Windley, B. F.; Coward, M. P.; Cooper, D. J. W.; Rex, A. J.; Rex, D.; Li, T.; et al. 1987. The closing of Tethys and the tectonics of the Himalaya. Geol. Soc. Am. Bull. 98:678–701.

Singh, A. K. 2013. Petrology and geochemistry of abyssal peridotites from the Manipur Ophiolite Complex, Indo-Myanmar Orogenic Belt, northeast India: implication for melt generation in mid-oceanic ridge environment. J. Asian Earth Sci. 66:258–276.

Sinha, A. K., and Mishra, M. 1992. Emplacement of the ophiolitic mélange along continental collision zone of Indus Suture Zone in Ladakh Himalaya. J. Himal. Geol. 3(2):179–189.

———. 1994. The existence of oceanic islands in the Neotethys: evidence from Ladakh Himalaya, India. Curr. Sci. 67:721–727.

Shah, S. K., and Sharma, M. L. 1977. A preliminary report on the fauna in radiolarites of the ophiolite-melange zone around Mulbekh, Ladakh. Curr. Sci. 46:817.

Sharma, K. K. 1989. Tectonic evolution of northwestern Himalaya: fission track age constraint. *In* Int. Geol. Cong., 28th (Washington, DC, 1989), Abstr. 3:84–85.

Sharma, M., and Wasserburg, G. J. 1996. The neodymium isotopic compositions and rare earth patterns in highly depleted ultramafic rocks. Geochim. Cosmochim. Acta 60:4537–4550.

Snow, J. E., and Dick, H. J. B. 1995. Pervasive magnesium loss by marine weathering of peridotite. Geochim. Cosmochim. Acta 59:4219–4235.

Srikantia, S. V., and Razdan, M. L. 1980. Geology of part of central Ladakh Himalaya with particular reference to Indus tectonic zone. J. Geol. Soc. India 21: 523–545.

———. 1985. The Indus tectonic zone of the Ladakh Himalaya: its geology, tectonics and ophiolite occurrence. Geol. Surv. India Rec. 115:61–92.

Sun, S. S., and McDonough, W. F. 1989. Chemical and isotopic systematics of oceanic basalts; implications for mantle composition and processes. *In* Saunders, A. D., and Norry, M. J., eds. Magmatism in the ocean basins. Geol. Soc. Lond. Spec. Publ. 42:313–345.

Taylor, R. N., and Nesbitt, R. W. 1988. Light rare-earth enrichment of supra subduction-zone mantle: evidence from the Troodos ophiolite, Cyprus. Geology 16: 448–451.

Treloar, P. J., and Rex, D. C. 1990. Cooling and uplift histories of the crystalline thrust stack of the Indian Plate internal zones west of Nanga Parbat, Pakistan Himalaya. Tectonophysics 180:32–349.

You, C. F.; Castillo, P. R.; Gieskes, J. M.; Chan, L. H.; and Spivack, A. J. 1996. Trace element behavior in hydrothermal experiments: implications for fluid processes at shallow depths in subduction zones. Earth Planet. Sci. Lett. 140:41–52.

Zhou, M. F.; Robinson, P. T.; Malpas, J.; and Li, Z. 1996. Podiform chromitites in the Luobusa ophiolite (southern Tibet): implications for melt-rock interaction and chromite segregation in the upper mantle. J. Petrol. 37:3–21.